

# Final Technical Report

---

*Award No. G15AP00053*

*Title:* Characterization of earthquake sources in near-real time along the Alaska-Aleutian subduction zone using continuous seismic and high rate GPS data

*Term:* April 1, 2015 – March 30, 2016

*Authors:*

Natalia A. Ruppert, Geophysical Institute, University of Alaska Fairbanks, 903 Koyukuk Drive, Fairbanks, Alaska, 99775-7320, tel. 907-474-7472, email [naruppert@alaska.edu](mailto:naruppert@alaska.edu)

Kenneth Macpherson, National Tsunami Warning Center, NOAA, 910 S Felton Street, Palmer, Alaska 99645, tel. 907-745-4212, email [Kenneth.macpherson@noaa.gov](mailto:Kenneth.macpherson@noaa.gov)

Jeffrey Freymueller, Geophysical Institute, University of Alaska Fairbanks, 903 Koyukuk Drive, Fairbanks, Alaska, 99775-7320, tel. 907-474-7286, email [jfreymueller@alaska.edu](mailto:jfreymueller@alaska.edu)

## 1. Abstract

We have implemented a continuous seismic moment tensor scanning algorithm at the Alaska Earthquake Center. This algorithm is capable of simultaneously estimating an earthquake's hypocenter, moment magnitude, and mechanism within a few minutes of the origin time and without analyst intervention. In order to implement the algorithm, we have developed a software package for the Antelope seismic system (BRTT, Inc.). This makes continuous moment tensor scanning technology available to any seismic observatories that utilize the Antelope processing system. We have tested the software on both synthetic and real data, both retrospectively and in real time, and find that it is an effective tool for rapidly characterizing the source of moderate earthquakes in Alaska.

## 2. Report

### 2.1. Introduction

While all seismic observatories routinely determine hypocentral location and a magnitude within a few minutes of an earthquake's occurrence, the ability to estimate seismic moment and sense of slip in a similar time frame remains less widespread. The earthquake size and mechanism, however, are critical parameters for rapid hazard assessment; for larger events, moment magnitude is more reliable due to the tendency of other magnitude scales to saturate, and certain mechanism types such as off-shore thrust events might indicate earthquakes with tsunamigenic potential. Therefore, there is a need for regional networks with access to real-time data to produce rapid and reliable moment tensor solutions for seismically active areas.

The state of Alaska is by far the most seismically active in the United States, with three quarters of all US earthquakes occurring in the state. The seismotectonics of the region are dominated by the Alaska-Aleutian subduction zone, which has produced some of the largest earthquakes ever recorded, including the 1964 M9.2 Great Alaska and 1965 M8.7 Rat Islands earthquakes [Frohlich, 1979]. The state also sees significant seismicity far inland from the subduction zone, including large continental earthquakes such as the 2002 M7.9 Denali Fault earthquake, which was the North American largest continental earthquake in 150 years [Eberhart-Phillips et al., 2003]. The Queen Charlotte fault system in southeastern Alaska is also highly active and most recently produced a M7.5 earthquake in 2013 [Yue et al., 2013]. These high rates of seismicity pose a significant hazard to the population and infrastructure of the state of Alaska. The tsunami precipitated by the 1964 Great Alaska earthquake resulted in severe damage and casualties, while the Trans-Alaska pipeline traverses several well-known faults and was lightly damaged in the 2002 Denali Fault event. More recently, a moderate M6.0 earthquake struck southeastern Alaska near the community of Gustavus on July 25, 2014. Although the ground motions for this event were light, it triggered a turbidite that severed a submarine fiber-optic cable, disrupting communications in the area. Because of the extent hazard, emergency managers in the state, as well as the public, require timely information about seismic activity, in order to help mitigate effects.

The Alaska Earthquake Center (AEC) is the primary source of definitive earthquake information for the state of Alaska. The Center receives and processes data from over 400 stations located throughout the state, from the far western Aleutians to the Arctic. Data types consist of a combination of broadband, short period, and strong motion sensors. Recently, AEC has been reporting in excess of 30,000 earthquakes per year in the state; an average of five per year are equal to or in excess of M6.0. The state has experienced eight M7.0 since 2010. The mission of the AEC is to help mitigate risk in Alaska by rapidly providing earthquake information to the public and stakeholders. The rapid determination of the seismic moment tensor for moderate events would further the AEC's mission by allowing the center to release the seismic moment and mechanism along with the customary hypocenter and magnitude parameters. In order to develop this capability, we have implemented a continuous moment tensor scanning algorithm at the AEC.

## **2.2. Continuous moment tensor scanning**

The theory of continuous moment tensor scanning of the long-period wavefield was originally formulated by Kawakatsu [1998]. He envisioned the process as using seismometers as machines to correlate the long-period ( $T \geq 20$  seconds) observed wavefield with the wavefield predicted by a grid of potential sources. This is accomplished by constructing a three dimensional (3D) grid of potential source points over the area to be monitored, and then choosing a sparse network of 3 or 4 robust stations in or near the monitoring grid. An example monitoring grid for southern Alaska is shown in Figure 1. If the velocity structure is known, Green's functions may be computed for every unique source-receiver combination in advance of any moment tensor calculation and stored in a computer

array  $G^{sr}$  for source  $s$  and receiver  $r$ . Then the observation equation relating the moment tensor to the data is given by

$$d_i^r(t) = \sum_{j=1}^P G_{ij}^{sr}(t) m_j^s + e_i^r \quad (1)$$

where  $d_i^r(t)$  denotes 3-component data at station  $r$  and component and trace  $i$ ,  $G^{sr}$  is the matrix of Green's functions between the source  $s$  and receiver  $r$ , and the  $m_j^s$ 's are the 6 independent elements of the moment tensor ( $P=6$ ). This equation may be solved via standard least-squares minimization of  $\frac{\partial}{\partial m} \sum_{i=1}^D e_i^2 = 0$ , leading to the following normal equations,

$$\sum_{j=1}^P \sum_{i=1}^D G_{ik}^{sr}(t) G_{ij}^{sr}(t) m_j^s = \sum_{i=1}^D G_{ik}^{sr} d_i^r(t)$$

or more succinctly in vector notation,

$$G^T G m^s = G^T d^r$$

The least squares solution of these normal equations is given by,

$$m^s = [(G^T G)^{-1} G^T] d^r \quad (2)$$

which is the correlation of the theoretical Green's functions with the data [Guilhem & Dreger, 2011; Guilhem et al., 2013]. The powerful aspect of this inversion scheme is that since the  $G^{sr}$  arrays are functions of the source-receiver geometry, which is known *a priori*, the time consuming tasks of computing Green's functions and the generalized linear inverses (GLI), may be performed in advance, before streaming any data. The calculation of the moment tensor then becomes as simple as taking the product of the GLI array and a segment of streamed data.

The correlation described by equation 2 is performed for every grid point at every time step (usually every 1 or 2 seconds) and the variance reduction is monitored via,

$$VR = \left[ 1 - \frac{\sum_{i=1}^D \sqrt{(data_i - synthetic_i)^2}}{\sum_{i=1}^D \sqrt{data_i^2}} \right] \times 100 \quad (3)$$

for every trace  $i$ . If there is no earthquake activity, the variance reductions will be low. However, once an earthquake occurs, the variance reduction will rise, and if it exceeds a certain threshold, an earthquake detection may be assumed. At this point, the algorithm had simultaneously computed the event's hypocenter, moment, and mechanism, all within a few minutes of the event origin time.

### 2.3. Software

The continuous moment tensor scanning concept has been implemented in real-time and with success at the University of Tokyo, the University of California Berkely, and Academia Sinica in Taiwan. The software used to implement the

algorithm is largely dependent on the acquisition system used by the respective networks. For example, the University of California Berkley uses the USGS Earthworm suite of tools for acquisition, so their implementation of the algorithm is accomplished via a C software package, called GridMT, that utilizes Earthworm libraries. The AEC uses the Antelope Environmental Monitoring Software (BRTT, Inc.) for acquisition and archiving, and so the technical crux of implementing the algorithm was the development of a GridMT software package for Antelope. Antelope consists of an integrated suite of programs for the collection, archiving, and processing of seismic data. The software is open-architecture, has been steadily developed for decades, and is in use at seismic observatories around the world. It provides an ideal environment for a project of this type, as it includes well-documented interfaces for software development.

When we set-out to develop our GridMT, the primary goal was to create a robust moment tensor scanner that could run for years with little maintenance required. In order to meet this goal, the code needed to be well-documented, easy to maintain, and relatively simple to set up; in short, the code needed to be “user-friendly”, and we have developed tools around the core scanner that enhance usability. All of the tools developed for this software package are documented via formal manual pages that are installed on the user's system during compilation. The code only uses Antelope libraries in addition to standard and readily available C and Python libraries. The code does not utilize any third part software such as the Seismic Analysis Code.

An overview of our Antelope GridMT software is shown in Figure 2. The nature of the algorithm is that the cumbersome and computationally expensive work of computing the GLI's is performed “offline” before streaming any data. Since speed is not essential for this task, we wrote a module for setting-up monitoring grids and computing GLI's in Python. This code, called 'gridgli', finds the geographic coordinates of all potential source points to be used in the grid, finds all source-receiver offsets and back azimuths, and displays a map of the grid for the user to evaluate. The code then loads the required Green's functions for the grid from an Antelope database, filters using the appropriate bandpass, constructs synthetic seismograms and computes the GLIs for all grid points. All of this computed information is written to files in formats required for the moment tensor scanner. The “gridgli” code is configured via a standard Antelope parameter file, a text file containing parameters in name-value pairs, where the pairs may be arrays. The user needs only to define a few parameters such as geographic extent of the grid, grid spacing, seismic station names, and a string defining the filter to be used. It takes a few minutes to edit the parameter file, then on the order of 40 minutes for the code to run for a 10-degree square grid using a modest desktop hardware. The only caveat to the ease of use of this program is the fact that the user must provide a database of Green's functions. This database must contain the 10 fundamental fault traces for every unique depth-distance combination. At the AEC, our strategy is to compute large databases containing Green's functions for all integer distances from 5 kilometer (km) to 900 km so that a single database will be sufficient for nearly every grid that may be computed. The database needs to be changed only if using a

different velocity model. Although providing this database places a burden on the user, it does allow them flexibility in how Green's functions are computed.

The core moment tensor scanner is called 'gridmt' (see Figure 2), and is written in C in order to exploit the computational efficiency of a compiled language. This code reads all of the files written by 'gridgli', including the GLI files and geometry information. It then loads Green's functions from the same database used to compute the GLI's, constructs synthetics to compare to the data in order to track variance reduction. After this start-up procedure, which takes a few minutes to accomplish, the code begins reading data, which is supplied to 'gridmt' via one of two 'skins'. The real-time version, called 'orbgridmt', reads data from a ring buffer and then passes the data to 'gridmt' without the need to write any files to a hard drive. The 'off-line' skin, called 'dbgridmt', reads data directly from a standard Antelope database of wave form data. This 'off-line' skin was originally developed in order to conveniently test the 'gridmt' code. However, we think of a this code also has efficacy for processing long time series of data in order to automatically produce moment tensor catalogs. Once the 'gridmt' code has ingested a segment of data of user-defined length, it begins correlating the data with the GLI and examining the variance reduction at every grid point. Upon completing the correlations for the entire grid, it reads an additional second of data, slides the correlation window along the data segment by one second, and then begins correlating again. If 'gridmt' finds a grid point where the variance reduction exceeds the user-defined threshold, it announces a detection. The code then outputs the best-fitting moment tensor solution by appending an output database with a moment tensor row. It also outputs a specially formatted ASCII solution file that may be visualized using included Python plotting tools, 'plot\_fit', and 'plot\_fit\_comb'. These tools are designed to make it easy to rapidly produce a publishable figure that could be used in an information release or pushed to social media.

## 2.4. Real-time data processing

A challenging element of implementing continuous moment tensor scanning is real-time data processing. The 'gridmt' code requires incoming data to be 1 sample per second (sps), so there must either be 1 sps channels available, or data must be decimated "on the fly". This is challenging, and the current version of the code does not have this capability. All Alaska network (AK) stations have 1 sps channels, so we only utilize these channels as input for GridMT. Antelope will soon have the ability to re-sample real-time data, so this restriction will be removed in later versions. We do implement a real-time Butterworth filter on the data, with a pass band between 25 seconds (s) and 50 s. This pass band is effective for moment tensor inversion for moderate regional earthquakes [Dreger, 2003]. We do not employ instrument deconvolutions, as this is challenging in real time, and sensors on in the AK network have a flat response in the 25 – 50 s pass band. We are experimenting with pre-convolving the Green's functions with the instrument responses, as this would remove the need for real-time deconvolutions.

For real-time scanning, it is essential that GridMT not fall behind the data stream, so that the rapid solutions arrive in a timely fashion. At the AEC, we configure 'gridmt' to read 380 s of data before beginning to compute correlations.

This length of data segment works well when inverting for regional events in the described frequency range, but does mean that moment tensor solutions will be at least 6 minutes behind the origin time. Unfortunately, we found that, using modest hardware on 10 degree grids, we require around 1.6 s to process 1 s of data. In order to prevent the code from falling-behind the data stream, we simply invert every 2 s.

## 2.5. Results

There are currently 3 monitoring grids operating in real-time in the state Alaska and these are shown in Figure 3. Each monitoring grid has a roughly 10-degree square extent, with grid spacing of 30 km in the latitude direction and 45 km in the longitude direction. The grids have a depth extent of 200 km, with 5 km vertical spacing in the crust and 20 km spacing in the mantle. Each grid uses 3 broad band stations with 1 sps channels for monitoring that were chosen for their long term robustness. The Aleutian grid covers a large segment of the Aleutian-Alaska subduction zone where tsunamigenic earthquakes are possible [Davies et al., 1981]. The south-central grid also covers a segment of the subduction zone, as well as the city of Anchorage, the largest in the state. The final grid covers a large area of central Alaska and includes the city of Fairbanks, the second largest in the state, and several prominent seismic zones, including a large portion of the Denali fault. There have been more than 250 earthquakes with  $M_L \geq 4.5$  in these 3 regions since 2005. Green's functions for the 3 grids were computed using the frequency-wavenumber code FKRRPROG with 1D velocity models [Saikia, 1994]. The velocity models used for each grid are the models used by the AEC for routine earthquake locations in the 3 respective regions.

We tested our GridMT using the 'dbgridmt' offline version to evaluate the algorithms performance. First we ran the code on synthetic wave forms, constructed by convolving source-time functions with Green's functions for a source location in the south-central grid. For this synthetic test, the GridMT best-fit solution resulted in a variance reduction of over 94% (Figure 4). The hypocenter and magnitude were recovered almost exactly, while the mechanism parameters were approximated to within a few degrees.

We further tested GridMT by running 'dbgridmt' on real data. For this test, we chose a moderate earthquake ( $M_L=5.8$ ) that occurred west of Anchorage, Alaska at 14:32 Alaska Daylight Time (AKDT) on June 24, 2015. This event occurred at intermediate depth and induced neither damage nor casualties. However, it was widely felt in south-central Alaska and generated significant public interest. The National Earthquake Information Center (NEIC) released a moment tensor solution for the event, allowing us the opportunity to compare a GridMT-generated solution with solution obtained via more conventional means. Using the same monitoring grid and network configuration that was used with the synthetic test, 'dbgridmt' produced the solution shown in Figure 5 with a 58% variance reduction. The GridMT-generated location, depth, and mechanism are very similar to the NEIC solution. We stress that these results were obtained automatically by the algorithm using just 3 stations, and provide a reasonable simulation of how the algorithm is expected to perform in real time.

After these successful tests using 'dbgridmt' to simulate real-time operation, we initiated real-time scanning for the Aleutian and the south-central monitoring regions using 'orbgridmt' in December 2015. To date there have been a handful detections each month. A result for  $M_L=4.9$  earthquake on April 29, 2016 in Kenai Peninsula region is shown in Figure 6. While the resulting magnitude  $M_w$  matches perfectly, the source mechanism is slightly different from the 1<sup>st</sup> motion solution. An Aleutian earthquake example from March 27, 2016 is shown in Figure 7. Again, the magnitude match is satisfactory, while the moment tensor mechanism is slightly different from that determined by NEIC and GCMT via conventional inversion methods.

## 2.6. Conclusions

The ability to rapidly compute earthquake moment tensors allows seismic observatories to release information that, in addition to being of interest to the public and scientists, may have the potential to mitigate hazard. Continuous moment tensor scanning of the long-period wave field is a technique for estimating a moderate earthquake's hypocenter, moment magnitude, and mechanism by correlating observed wave forms with predicted wave forms from a grid of potential sources. This source estimation is accomplished within a few minutes of the earthquake's origin time without analyst intervention.

In order to implement continuous moment tensor scanning at the AEC, we developed a GridMT code for use with the Antelope seismic software. The code also includes a retrospective scanner that reads from databases that is useful for automatically processing stored data to produce a moment tensor catalog. This code, in addition to an efficient moment tensor scanner written in C, includes Python codes for grid set-up and output visualization.

In terms of accuracy, continuous moment tensor scanning algorithms, which usually use a small number of stations, cannot compete with more conventional methods that may use many stations, full wave form inversion schemes, and cross-correlations to align wave forms. However, our GridMT algorithm has produced rapid, reasonable accurate solutions for moderate ( $5 \leq M_L \leq 7$ ) events in Alaska. Further work is required to extend the ability of the algorithm to compute moment tensors for larger magnitude earthquakes. This can be accomplished by scanning the wave field at longer periods in order to make the point source assumption more valid, and by incorporating different data types such as strong motion and high-rate GPS to avoid the problem of broad band instruments going off scale. The flexibility provided by the current code makes it easy to use the appropriate Green's functions for these different data types. Modifications such as these have the potential to transform continuous moment tensor scanning from a tool for rapid information release to a source of tsunami warning information.

## 2.7. References

- Davies, J.; Sykes, L.; House, L. and Jacob, K. (1981). *Shumagin Seismic Gap, Alaska Peninsula: History of great earthquakes, tectonic setting, and evidence for high seismic potential*, Journal of Geophysical Research: Solid Earth 86 : 3821-3855.
- Dreger, D. S., Lee, W. K., K. H. J. P. C. & Kisslinger, C. (Ed.), **2003**. *TDMT\_INV: Time Domain Seismic Moment Tensor INVersion*. In: *International Handbook of Earthquake and Engineering Seismology*. , .
- Eberhart-Phillips, D.; Haeussler, P. J.; Freymueller, J. T.; Frankel, A. D.; Rubin, C. M.; Craw, P.; Ratchkovski, N. A.; Anderson, G.; Carver, G. A.; Crone, A. J.; Dawson, T. E.; Fletcher, H.; Hansen, R.; Harp, E. L.; Harris, R. A.; Hill, D. P.; Hreinsdóttir, S.; Jibson, R. W.; Jones, L. M.; Kayen, R.; Keefer, D. K.; Larsen, C. F.; Moran, S. C.; Personius, S. F.; Plafker, G.; Sherrod, B.; Sieh, K.; Sitar, N. and Wallace, W. K. (2003). *The 2002 Denali Fault Earthquake, Alaska: A Large Magnitude, Slip-Partitioned Event*, Science 300 : 1113-1118.
- Frohlich, C. (1979). *An efficient method for joint hypocenter determination for large groups of earthquakes* , Computers & Geosciences 5 : 387 - 389.
- Guilhem, A. and Dreger, D. S. (2011). *Rapid detection and characterization of large earthquakes using quasi-finite-source Green's functions in continuous moment tensor inversion*, Geophysical Research Letters 38 : L13318.
- Guilhem, A.; Dreger, D. S.; Tsuruoka, H. and Kawakatsu, H. (2013). *Moment tensors for rapid characterization of megathrust earthquakes: the example of the 2011 M9 Tohoku-oki, Japan earthquake*, Geophysical Journal International 192 : 759-772.
- Kawakatsu, H. (1998). *On the realtime monitoring of the long-period seismic wavefield*, Bull. Earth. Res. Inst. 73 : 267-274.
- Saikia, C. K. (1994). *Modified frequency-wavenumber algorithm for regional seismograms using Filon's quadrature: modelling of Lg waves in eastern North America*, Geophysical Journal International 118 : 142-158.
- Yue, H.; Lay, T.; Freymueller, J. T.; Ding, K.; Rivera, L.; Ruppert, N. A. and Koper, K. D. (2013). *Supershear rupture of the 5 January 2013 Craig, Alaska (Mw 7.5) earthquake*, Journal of Geophysical Research: Solid Earth 118 : 5903-5919.

## 2.8. Figures

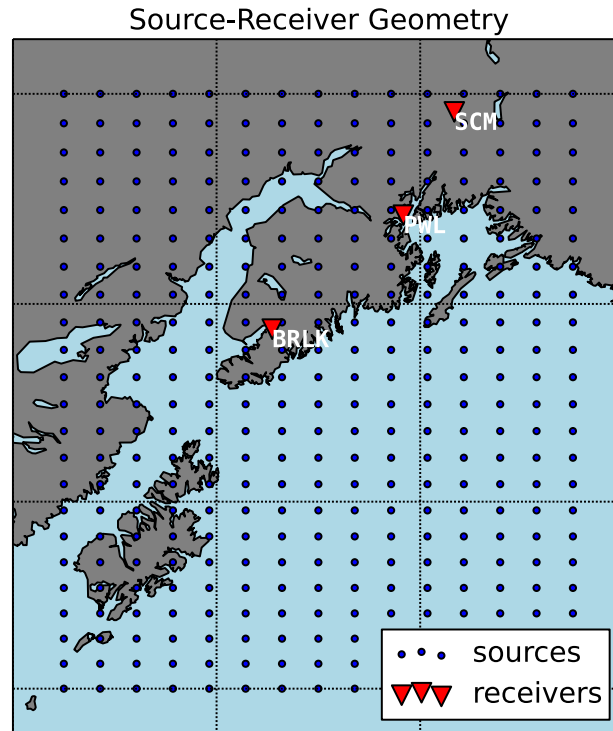


**Figure 1.** Example continuous moment tensor scanning grid for south-central Alaska. Receivers are broadband sensors from the Alaska network, while 'sources' are potential source points used for the computation of Green's functions.

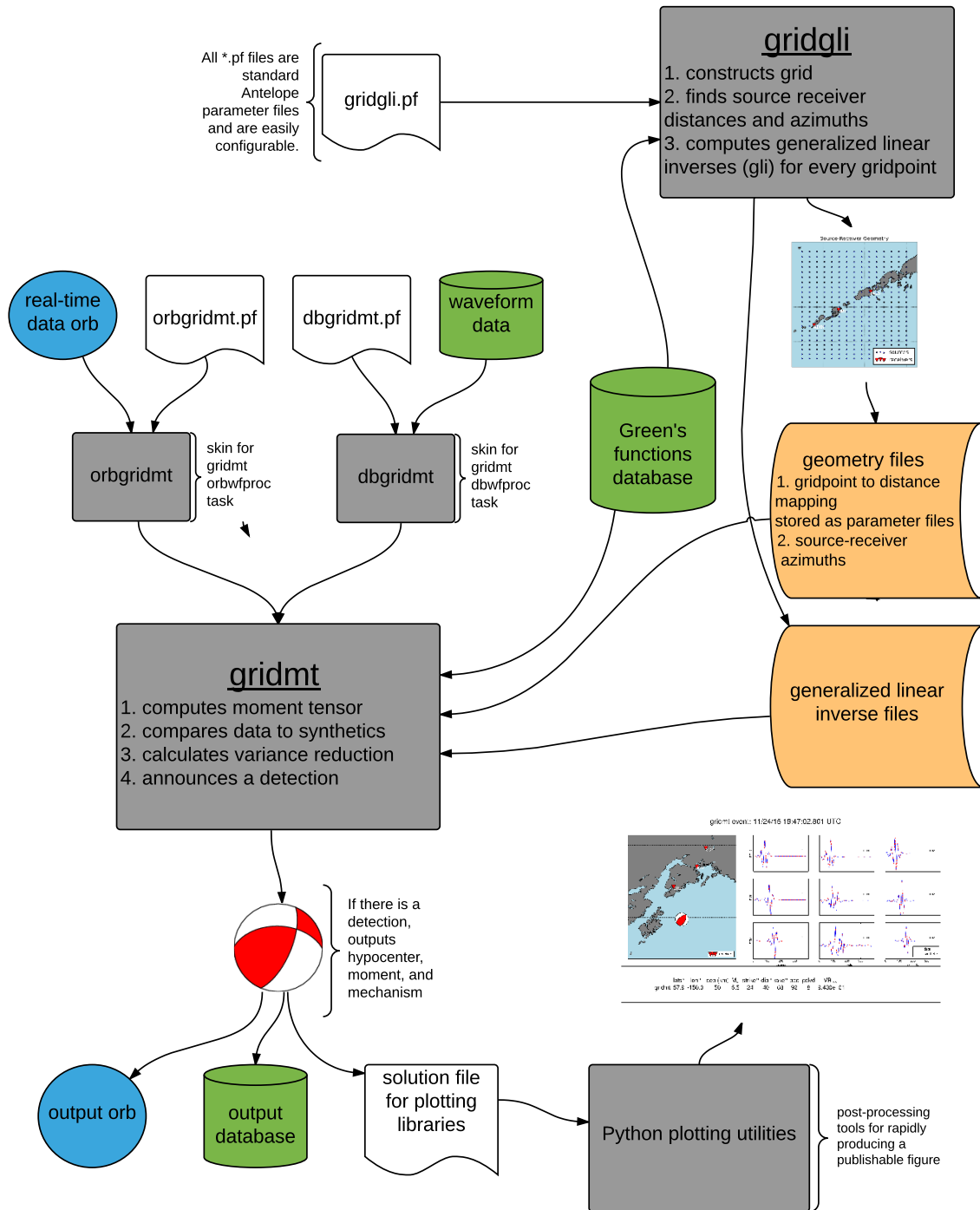


**Figure 2.** Overview of the continuous moment tensor scanning software developed at the Alaska Earthquake Center.

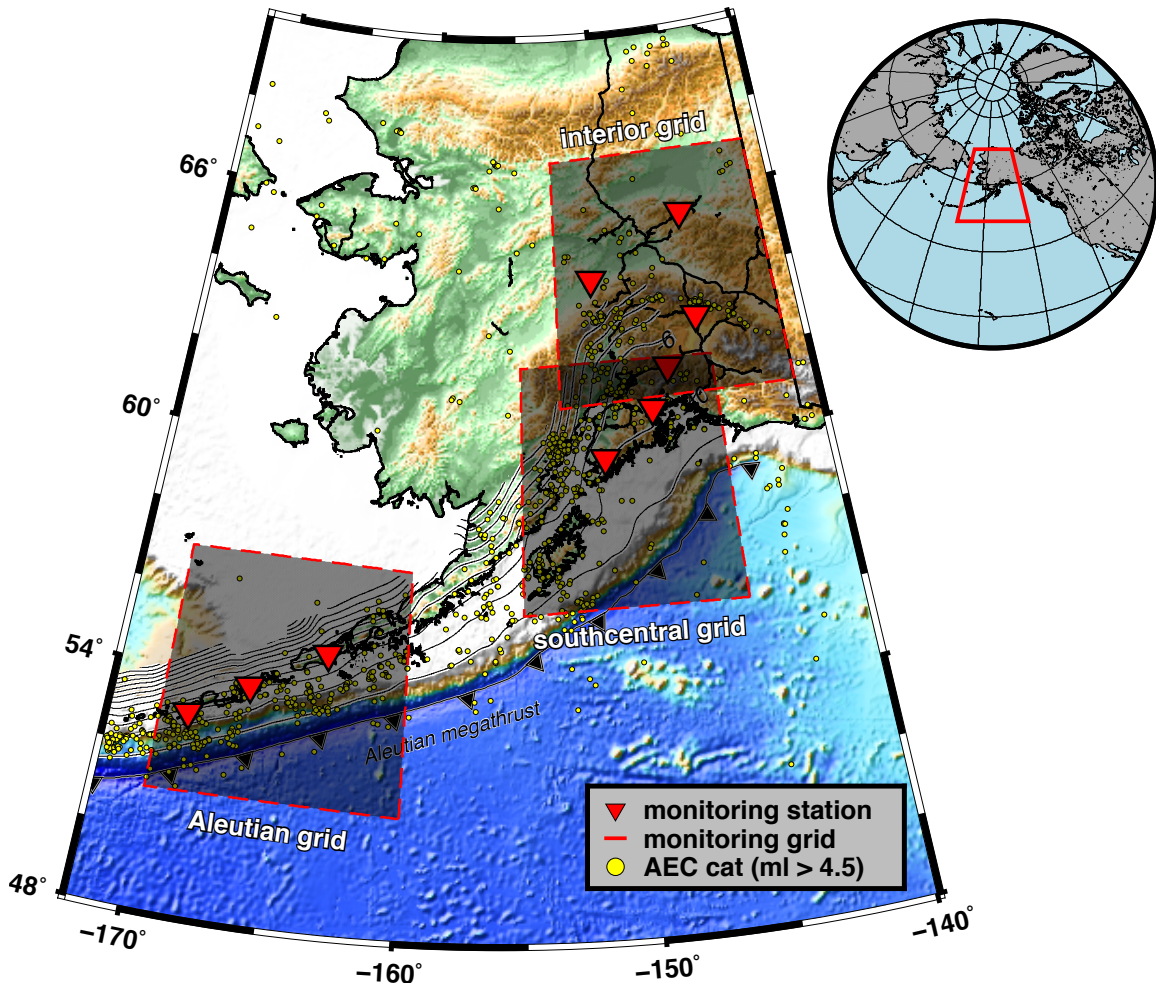


**Figure 3.** GridMT monitoring regions for the state of Alaska. The Aleutian grid cover a large area of the Aleutian megathrust where tsunamigenic earthquakes are possible. The Southcentral grid covers another section of megathrust and includes Anchorage, the largest city in the state. The interior grid covers the large town of Fairbanks, and notable seismic zones including the Denali fault. The hypocenters of events greater than 4.5 in the AEC catalog are shown as yellow dots.

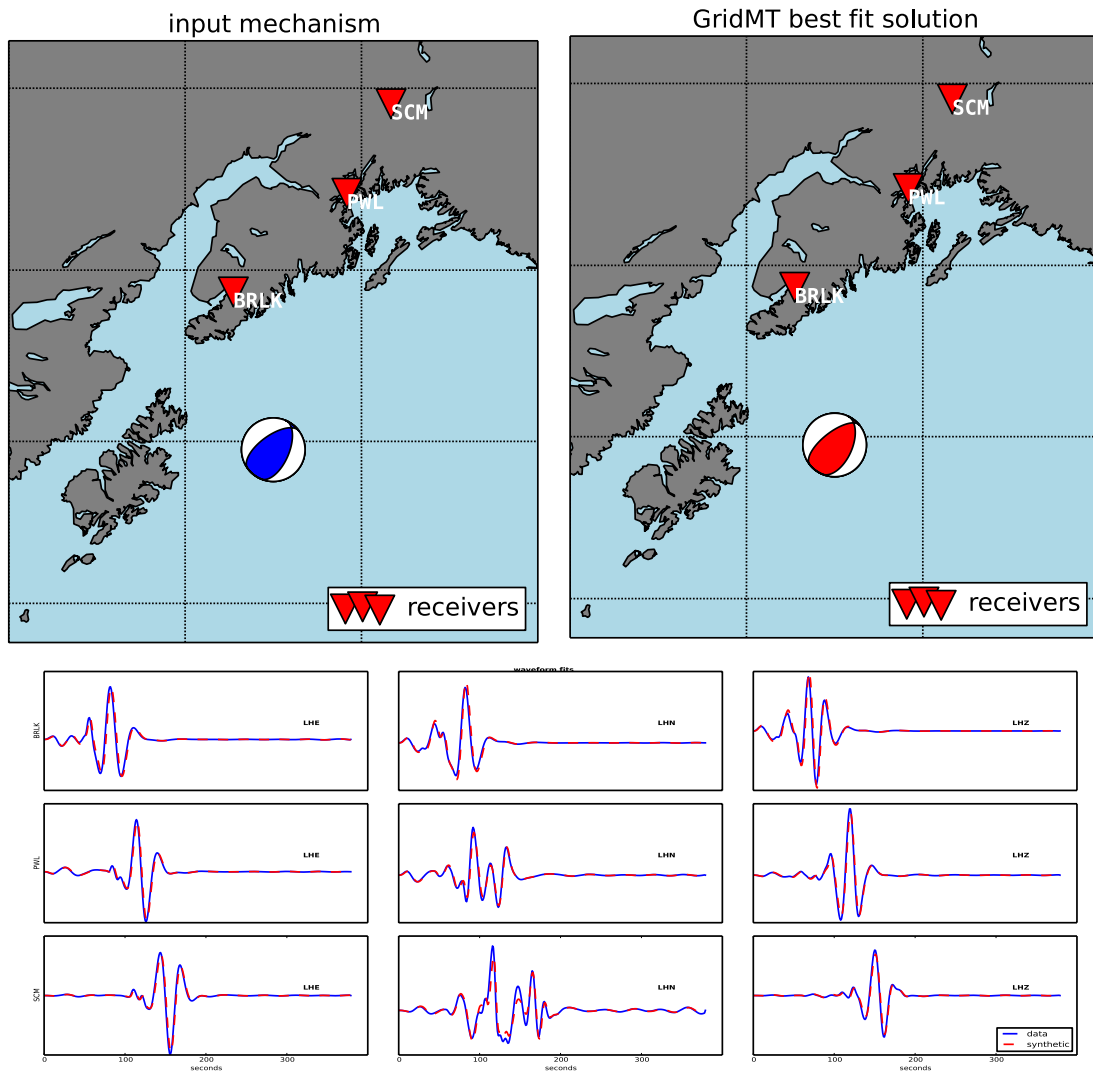
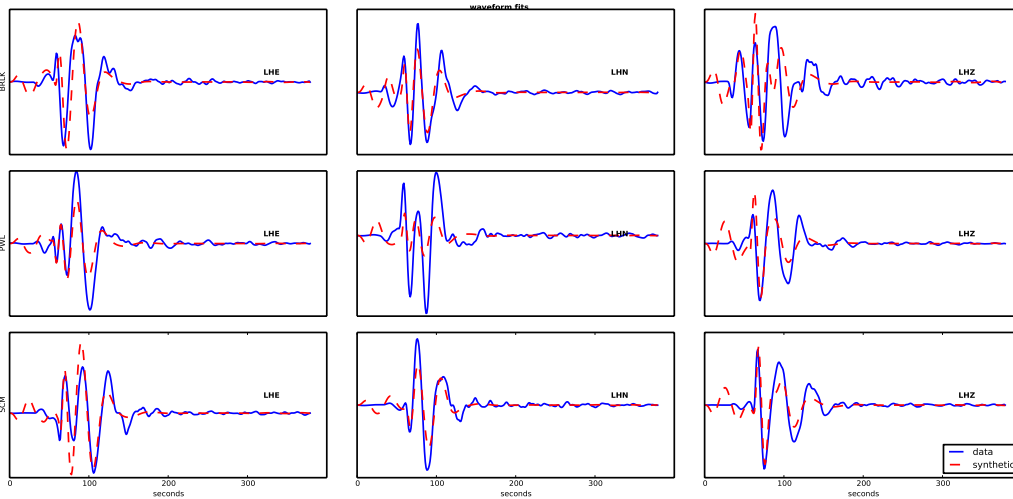
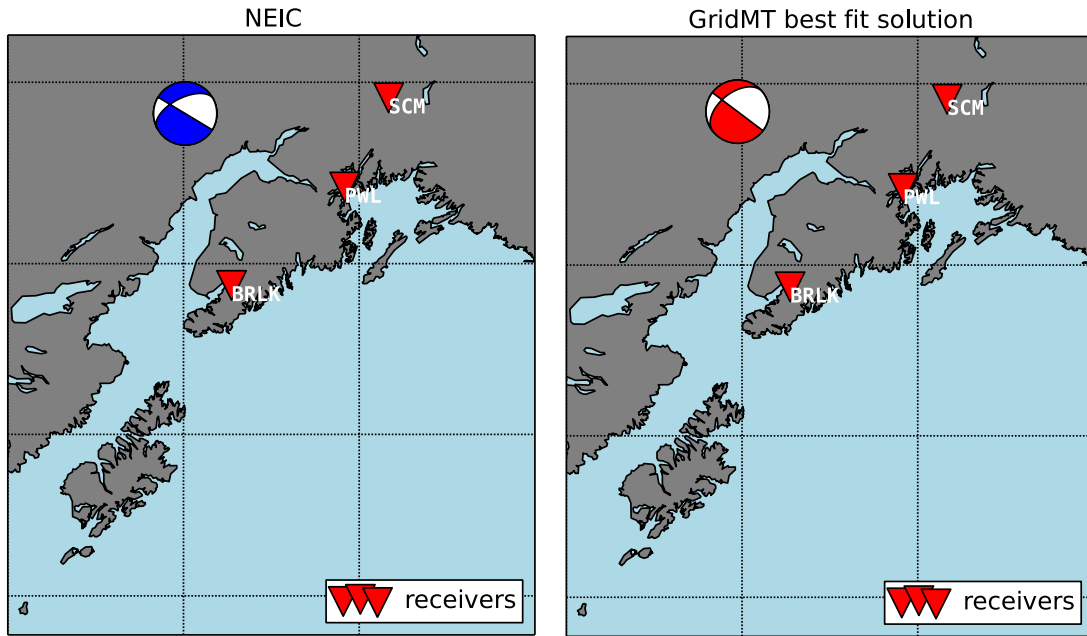


**Figure 4.** Result of running 'dbgridmt' on a synthetic moderate earthquake located near the center of the Southcentral monitoring grid. The top panels show the location and input mechanism on the right and the best-fit GridMT solution on the left. Waveform fits are shown in the middle panel, with the data plotted in blue and the best-fit synthetic in red. The parameters for the input hypocenter and mechanism and the GridMT-recovered output hypocenter and mechanism are summarized in the table at the bottom. The best-fit solution was associated with a variance reduction of 94%.



Solution	Lon (deg)	Lat (deg)	Depth (km)	Strike (deg)	Dip (deg)	Rake (deg)	Mw	DC %	CLVD %
NEIC	-151.96	61.66	114	307	56	109	5.77	100	0
GridMT	-151.1	61.7	110	301	53	118	5.8	65	35

**Figure 5.** Result of running 'dbgridmt' on a moderate ( $m_l \approx 5.8$ ) earthquake that occurred in south-central Alaska at 14:32 Alaska Daylight Time on June 24, 2015. The top panels show the location and moment tensor computed by the NEIC on the left and the best-fit GridMT solution on the right. Waveform fits are shown in the middle panel, with the data plotted in blue and the best-fit synthetic in red. The parameters for the NEIC hypocenter and mechanism and the GridMT-computed hypocenter and mechanism are summarized in the table at the bottom. The best-fit solution was associated with a variance reduction of 59%.

gridmt event: 4/29/16 08:23:48.177 UTC

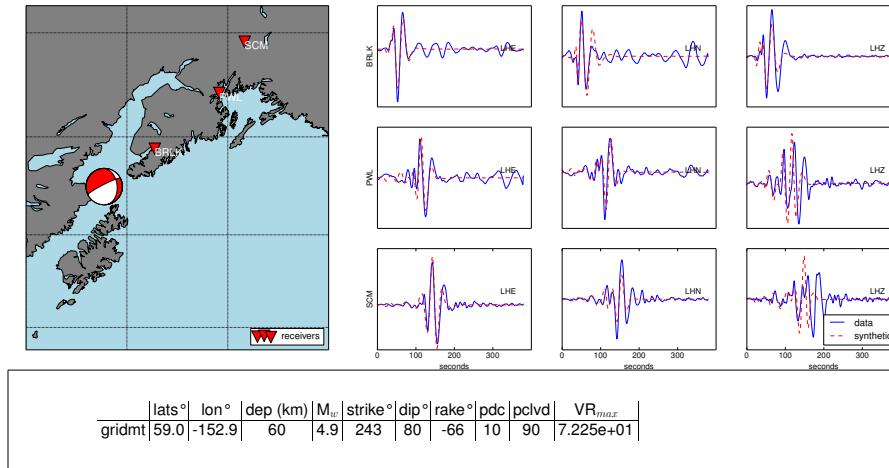


**Figure 6.** GridMT output for an event in southcentral Alaska.

gridmt event: 3/27/16 18:01:29.379 UTC

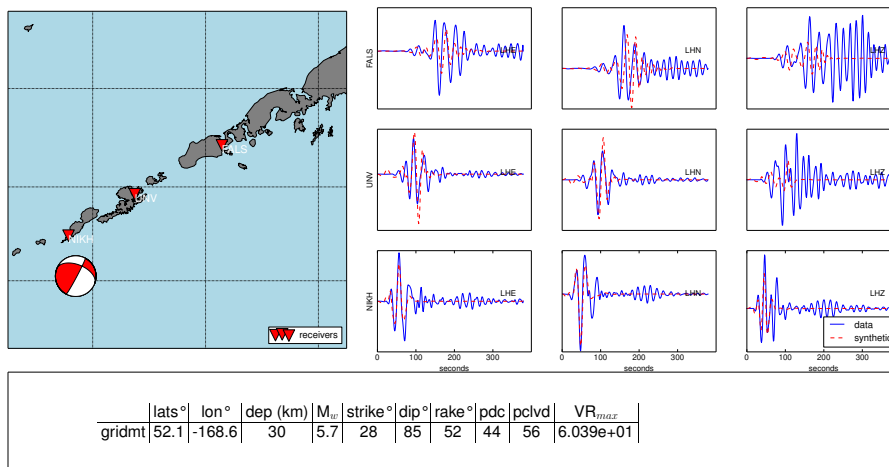


**Figure 7.** GridMT output for an event in Fox Islands.

### 3. Presentations

- K. Macpherson, K., Ruppert, N., Freymueller, J., Lindquist, K., Harvey, D., Dreger, D., Lombard, and Duilhem, A., *A real-time earthquake moment tensor scanning code for the Antelope system (BRTT, Inc)*, Poster, AGU Fall Meeting, December 14-18 2015, San Francisco, California.
- K. Macpherson, K., Ruppert, N., Dreger, D., Lombard, P., Freymueller, J., Nicolsky, D., and Duilhem, *Mainshock and aftershock mechanisms of the Mw=7.5 Craig, Alaska earthquake of January 5, 2013 from continuous moment tensor scanning*, Poster, SSA Meeting, April 30 – May 2 2014, Anchorage, Alaska.